Research Article

Cesium Salt of Sodium 30-Tungstopentaphosphate: An Effective and Green Polyoxometalate for Synthesis of Gold Nanoparticles along with Decoration of Titanium Dioxide with Gold Nanoparticles for Bleaching of Malachite Green

Fatemeh Farrash Bamoharram,[1] Afsaneh Moghadam Jafari,[1] Ali Ayati,[2] Bahareh Tanhaei,[2] and Mika Sillanpää[2]

[1] *Department of Chemistry, Mashhad Branch, Islamic Azad University, Mashhad 91735-413, Iran*
[2] *Laboratory of Green Chemistry, Department of Chemistry, Lappeenranta University of Technology, Sammonkatu 12, 50100 Mikkeli, Finland*

Correspondence should be addressed to Fatemeh Farrash Bamoharram; fbamoharram@gmail.com

For the first time, capability of the cesium salt of sodium 30-tungstopentaphosphate, the so-called Preyssler's anion (CsP_5), as a green and eco-friendly polyoxometalate was investigated in the synthesis of gold nanoparticles and decoration of titanium dioxide with gold nanoparticles. Gold nanoparticles and nanocomposites were characterized by TEM, XRD, UV, and FTIR. TEM images showed that the gold nanoparticles have tubular and spherical shapes and particle size ranges from 10 to 25 nm. For gold-decorated titanium dioxide/Preyssler, a comparison between pure and amine-modified titanium dioxide showed higher loading of gold nanoparticles on amine-functionalized titanium dioxide. The performance of CsP_5 was compared with its pure acid (HP_5). Our findings showed that CsP_5, as a catalytic linker to bind onto titanium dioxide surface for reducing gold nanoparticles, renders decoration better than HP_5 in both pure and modified titanium dioxide. In addition, efficiency of the photocatalytic bleaching of malachite green by the synthesized nanocomposites was found to be excellent.

1. Introduction

The recent advances in green catalysis, particularly when coupled with modifying of inorganic materials, have opened new avenues for the catalytic technology. One of the most important inorganic materials is titanium dioxide and different applications of it have been discovered in many fields, including photovoltaics [1, 2], photocatalysis [3, 4], self-cleaning coatings [5], and photoelectrocatalytic degradation of organic compounds [6, 7].

But, despite these large range of applications, the application of these particles is limited by the challenge of electron-hole recombination and their band-gap energy of 3.2 eV [8], which requires exposure to ultraviolet light for photocatalytic applications. For overcoming the electron-hole recombination phenomenon, many researchers have made an attempt to shift the band-gap energy of titanium dioxide toward the visible region [9–11] and used doping with small amounts of transition metals [12, 13].

To this end, titanium dioxide has been decorated with metals and metal oxides through chemical or photodeposition methods [14–23].

However, in deposition of metal nanoparticles on titanium dioxide surface, the final product contains a mixture of both metal nanoparticles and metal-decorated titanium dioxide. A possible solution to overcome this problem could be based on the immobilization of a reducing agent on the surface of titanium dioxide particles.

Polyoxometalates can reduce easily without any change in the structure and the reduced form of them bound to titanium dioxide can act as a reducing agent for metal ions to decorate metal nanoparticles, specifically on titanium

dioxide surfaces [24]. Pearson and coworkers demonstrated decoration of titanium dioxide with metal nanoparticles using Keggin as an efficient polyoxometalate [25]. In addition, polyoxometalates can reduce noble metals to prepare nanoclusters in the presence of light [26, 27]. Anyway, although there are many structural types of polyoxometalates, the majority of processes use the most common Keggin type, owing to its availability and chemical stability, and the role of Preyssler polyoxometalate, $[NaP_5W_{30}O_{110}]^{14-}$, has been largely overlooked.

The oval-shaped Preyssler polyoxometalate consists of a cyclic assembly of five PW_6O_{22} units, each derived from the spherical Keggin anion, $[PW_{12}O_{40}]^{3-}$, by the removal of two sets of three corner-sharing WO_6 octahedra. The $[XM_{12}O_{40}]^{n-}$ (Keggin structure) consists of one XO_4 tetrahedron surrounded by four M_3O_{13} sets linked together through oxygen atoms. The Preyssler's anion structure consists of five PO_4 tetrahedron surrounded by 30 WO_6 which are connected to each other by edge and corner-sharing oxygens. A sodium ion is located within the polyanion on the five-fold axis and 1.25 Å above the pseudomirror plane that contains the five phosphorus atoms.

The properties of polyoxometalates such as thermal stability as well as hydrolytic stability and catalytic activity are sensitive to their structures [28, 29]. In addition, the kind and number of counterions as well as their constituent elements have an important effect on the catalytic activity, chemical behavior, and the redox properties of the polyoxometalates. Due to these reasons, a different behavior and activity is expected for each polyoxometalate with a different structure. Among a wide variety of studied heteropolyacids (an important class of polyoxometalates) with different size and structures, there are only three anions, $[NaSb_9W_{21}O_{86}]^-$, $[NaAs_4W_{40}O_{140}]^{25-}$, and $[NaP_5W_{30}O_{110}]^{14-}$ that have been reported to encapsulate rare-earth ions [30–32]. The latter of these, Preyssler's anion, is one of the largest known polyanions and important advantages of this polyanion over the Keggin and Dawson heteropolyacids are (i) more thermal stability, (ii) more hydrolytic stability (pH = 0–12), (iii) larger number of counter cations, and (iv) larger number of metal atoms. These properties are very important in catalytic processes, especially when we work in acidic and basic conditions. For example, while Keggin and Dawson, $[X_2M_{18}O_{62}]^{n-}$, polyoxometalates are stable in pH = 1–3 and 1–6, respectively, the Preyssler is stable in pH = 0–12. Additionally, while the oxidation of organic substrates by hydrogen peroxide in the presence of Keggin proceeds via degradation of structure to an active peroxopolyoxometalate, the Preyssler catalyst catalyzes the reactions without any degradation of structure [33]. This is very important in catalytic reactions in the presence of hydrogen peroxide. The large anion with the larger number of metal atoms also provides many "sites" on the oval-shaped molecule that are likely to render the catalyst effective, better than Keggin and Dawson types.

In continuation of our works on applications of Preyssler acid, $H_{14}[NaP_5W_{30}O_{110}]$, in catalytic and photocatalytic reactions [34, 35] and cited references in [35] and extending the applications of Preyssler, and also due to the importance of metal-titanium dioxide decoration, it is highly relevant to

know what occurs if the Preyssler's anion joins with titanium dioxide and use it as a catalytic linker for reducing gold ions. In addition, it is also important to investigate the role of another polyoxometalates apart from Keggin heteropolyacids. We think the most important and credential part of our work is to introduce and establish nanocesuim salt of Preyssler type heteropolyacid, $Cs_{12}H_2[NaP_5W_{30}O_{110}]$, which can be applied as an efficient and competing nanocatalyst with those of Keggin type which have been already reported as bulk.

Also, another goal in this research was to answer this question: does counter cation in the Preyssler structure, which is responsible for primary, secondary, and tertiary structures, have an important role on loading of gold nanoparticles onto titanium dioxide?

To this purpose, in the present work, at first in continuation of our earlier works [36], we investigated the performance and capability of cesium salt of sodium 30-tungstopentaphosphate, $Cs_{12}H_2[NaP_5W_{30}O_{110}]$, in synthesis of gold nanoparticles and after that, we studied decoration of titanium dioxide with gold nanoparticles in the presence of the Preyssler with different counterions including Cs^+ and H^+. Interestingly, we have found that the Preyssler catalyst with Cs^+ as counterion not only can change shape and size of gold nanoparticles but also can lead to a higher loading of gold nanoparticles onto titanium dioxide. Also we have investigated the application of different forms of Preyssler nanocomposites for bleaching of malachite green.

2. Experimental

2.1. Materials and Methods. All of the chemicals were purchased from Merck and Sigma Aldrich Companies and used as received. FT-IR spectra were recorded with a Brucker scientific spectrometer (solid sample, KBr pellets). The synthesized nanostructures were characterized by Transmission Electron Microscopy (PHILIPS CM-120 and JEOL-2200FS FEG). A double beam spectrophotometer UV-Vis was used for UV-Vis analysis (OPTIZEN 3220).

2.2. Preparation of HP_5 and CsP_5. At first, 33 g $Na_2WO_4 \cdot 2H_2O$ was dissolved in 45 mL water by stirring; and then 25 mL of phosphoric acid 85% was added. The mixture was refluxed for 5 h. After that, 10 mL H_2O and 10 g KCl were added into the above mixture to form a light green precipitate. The green precipitate was obtained by filtration and washed successively by 2 M aqueous solution of CH_3COOK and methanol. Recrystallization in hot water led to formation of $K_{12.5}Na_{1.5}[NaP_5W_{30}O_{110}]$ in needle white color crystals.

Preyssler acid, $H_{14}[NaP_5W_{30}O_{110}]$ (HP_5), was prepared by the passage of a solution of the $K_{12.5}Na_{1.5}[NaP_5W_{30}O_{110}]$ in water through a column (50 cm) of Dowex 50WX8 in the H^+ form and evaporation of the elute to dryness under vacuum.

For the preparation of CsP_5, Preyssler acid and CsCl in a mole ratio of 1 : 14 were put into a mortar and several drops of surfactant Triton X-100 were added. The formed microcells in the solid state reaction owing to the interaction between

the crystal water of Preyssler and the triton-X-100 are metastable and provide reaction fields for the formation of nanoparticles. The mixture was ground for 50 min and after washing in an ultrasonic bath, the mixture was centrifuged. The synthesized nanoparticles dried in an oven for 4 h (50–60°C). The number of obtained Cs ions was 12, measured by ICP measurement and titration method. Preyssler acid is highly soluble in water but has lower surface area (0.78 m^2/gr) than acidic cesium salt of Preyssler (2.61 m^2/g).

2.3. Preparation of Titanium Dioxide-CsP$_5$ and Amine-Functionalized Titanium Dioxide-CsP$_5$.

The functionalized titanium dioxide is prepared as follows.

2.5 g of TiO$_2$ was suspended in 25 mL toluene and refluxed for 1 h; and then 1.25 g 3-aminopropyltriethoxy silane was added into the above mixture with further stirring for 24 h. The product was obtained by filtration, washed successively with toluene, ethanol, and water, and finally dried in vacuum at 80°C for 12 h.

Titanium dioxide-CsP$_5$ and amine-functionalized titanium dioxide-CsP$_5$ were synthesized by impregnating titanium dioxide (anatase, Aldrich, 232033) and functionalized titanium dioxide powders with an aqueous solution of the HP$_5$ or CsP$_5$. After stirring the mixture, the solvent was evaporated to dryness. The obtained powders were dried in an oven at 80°C.

2.4. Decoration with Gold Nanoparticles.

In two parallel experiments, a suspension of the obtained powders, titanium dioxide-CsP$_5$ and amine-functionalized titanium dioxide-CsP$_5$, (10 mg) was dispersed in an ultrasonic bath. After that, 5 mL HAuCl$_4$ (10^{-3} M) and 2 mL propan-2-ol were added to each solutions; and then it was irradiated under the high pressure of mercury lamp as UV light source. After 1 h, the suspensions were filtered, rinsed with water, and dried in a vacuum oven. The obtained nanocomposites were used in photocatalytic reactions.

2.5. Typical Procedure for Bleaching of Malachite Green.

In a typical reaction, 0.01 g photocatalyst was added to 100 mL of malachite green (10 ppm), sonicated for 10 min, and left for 15 min in a dark place. The mixture was irradiated in a photoreactor. The photoreactor was designed with an internal light source surrounded by a quartz jacket. The temperature of the suspension was maintained at 25°C by circulation of water through an external cooling coil. The optical path length was about 2 cm. The light source was a 125 W high-pressure mercury lamp. The suspension was illuminated from the top and at given irradiation time intervals, liquid samples were taken from the mixture and the absorbance of the malachite green solution was measured with a UV-Vis spectrophotometer.

3. Results and Discussion

Synthesis of gold nanoparticles was performed with a one-pot synthesis technique in the presence of Preyssler with Cs$^+$ as counterion. The used method is simple and efficient and takes place within a short time (15 min) at ambient temperature. Using Preyssler as a reducing agent and stabilizer, the synthesis of gold nanoparticles by photolysis of gold (III)/Preyssler/propan-2-ol solution was carried out.

Preyssler polyoxometalate (POM) plays the role of transferring electrons from propan-2-ol (S) to gold (III) and also stabilizing the nanoparticles (1). Consider

$$POM + S \longrightarrow POM\left(e^-\right) + S_{OX}$$
$$POM\left(e^-\right) + Au^{3+} \longrightarrow POM + Au^0$$
(1)
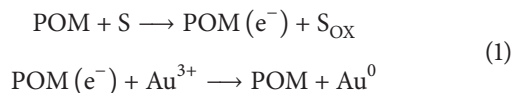
The morphology and size of gold nanoparticles were characterized by TEM. The TEM image is shown in Figure 1(b).

Interestingly, as we can see, counterions can affect both the size and the shape of the nanoparticles. So, when H$^+$ is a counterion, the shapes of the gold nanoparticles were nearly uniform hexagonal structures and the size of the synthesized gold nanoparticles varied from 13 to 43 nm (Figure 1(a)). When H$^+$ was replaced by Cs$^+$, interestingly, a mixture of tubular and spherical gold nanoparticles with the size of 10–25 nm was obtained (Figure 1(b)). With respect to the fact that Preyssler with Cs$^+$ could change morphology and size of gold nanoparticles, it is suggested that the tertiary structure type has an important effect in this catalysis process.

There are three classes of structures which we call the primary, secondary, and tertiary structures [29]. Heteropolyanions in the solid state are ionic crystals consisting of large polyanions (primary structure), cations, water of crystallization, and other molecules. This three-dimensional arrangement is the secondary structure. In addition to these two structures, the tertiary structure is very influential on the catalytic function of solid heteropolyanions. Counter cations greatly influence the tertiary structure of heteropolyanions, and the salts are classified by the size of cation into group A (small metal cations like Na and Cu) and group B (large metal cations like Cs, NH$_4$, etc.) [29]. So, we can conclude that the synthesis process can be controlled by tertiary structure of Preyssler. Also, from Figure 1, it is clear that there is no agglomeration. Usually there is a tendency of agglomeration via Coulomb or van der Waals forces in the synthesis process of nanoparticles [37]. Preyssler is an excellent stabilizer to prevent agglomeration. In addition, Preyssler is easily separated after the reaction and will not contaminate the gold nanoparticles.

Figure 2 shows UV-Vis absorption spectra of the synthesized gold nanoparticles. A surface plasmon resonance band of gold nanoparticles at about 530 nm appeared after 45 and 15 min, in the presence of HP$_5$ and CsP$_5$, respectively. UV-Vis analysis showed that in the presence of CsP$_5$, gold nanoparticles were synthesized in shorter time.

TEM micrographs of gold-decorated titanium dioxide-Preyssler with H$^+$ and Cs$^+$ as counterions are shown in Figure 3.

In comparison with HP$_5$, there is a higher loading of gold nanoparticles on titanium dioxide in the presence of CsP$_5$. Group B salts of polyoxometalates with larger metal ions like Cs$^+$ have higher surface area than group A. Thus, it is suggested that, because Preyssler acts as a localized reducing agent, a higher surface coverage with CsP$_5$ results
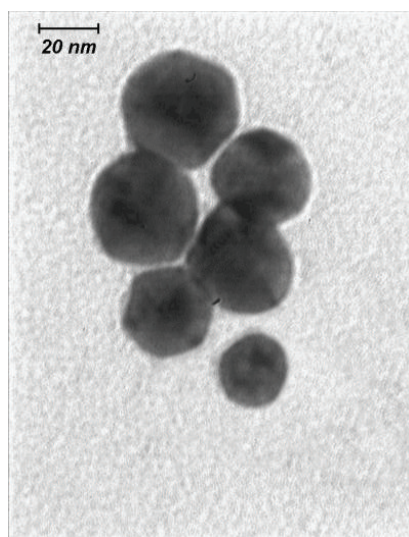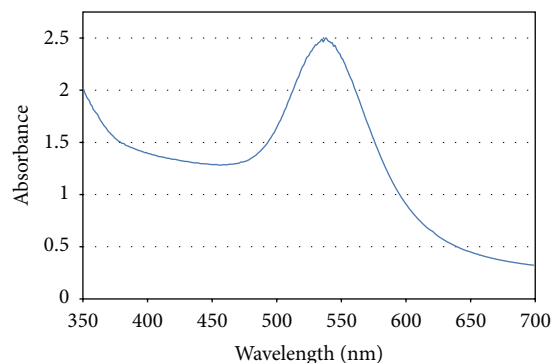
(a)
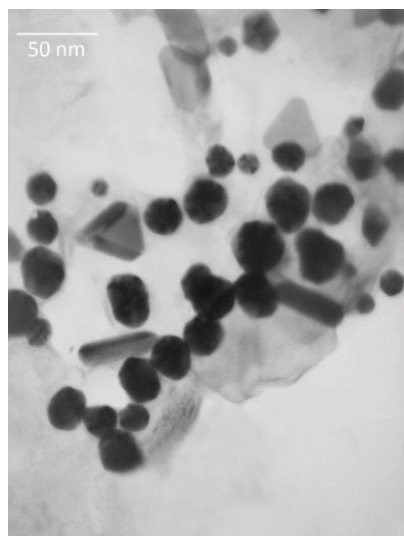
(b)

FIGURE 1: TEM images of the synthesized Au nanoparticles in the presence of HP_5^{36} (a) and CsP_5 (b).

(a)

(b)

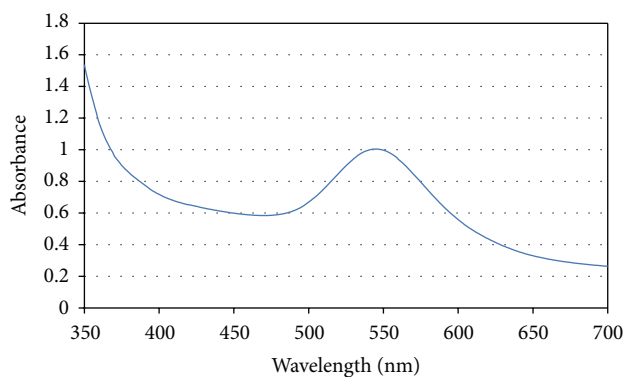FIGURE 2: UV-Vis spectra of the synthesized gold nanoparticles in the presence of HP_5 (a) and CsP_5 (b).

in enhanced reduction of $HAuCl_4$ to gold nanoparticles on titanium dioxide surface. The gold nanoparticles formed using HP_5 and CsP_5 are 2–10 and 20–50 nm, respectively.

TEM micrographs for decoration of the amine-functionalized titanium dioxide with gold nanoparticles are shown in Figure 4. This figure shows higher loading of gold nanoparticles on amine-functionalized titanium dioxide. This higher loading can be related to strong electrostatic interactions between negatively charged Preyssler polyoxometalate with positively charged amine-functionalized titanium dioxide. Interestingly, for amine-modified titanium dioxide, higher loadings were obtained in the presence of CsP_5 again. So, we can conclude that the tertiary structure in polyoxometalate, which led to a higher surface coverage, can control loading amounts.

Binding of Preyssler to titanium dioxide was confirmed by infrared spectroscopy as shown in Figure 5. Because

intermolecular interactions lead to a change in the frequencies of the metal-oxygen stretching bands, as well as the intensity and position of the corresponding IR bands, FTIR spectroscopy can be used to confirm the interaction of HPAs with different molecules [38].

Preyssler's structure gives rise to four types of oxygen that are responsible for the fingerprints bands of Preyssler anion between 1200 and 600 cm^{-1}. The characteristic bands of Preyssler structure, $[NaP_5W_{30}O_{110}]^{14-}$, are three bands due to P-O stretching at 1163 cm^{-1} (medium), 1079 cm^{-1} (medium), and 1022 cm^{-1} (weak), and two bands attributed to W-O-W at 941 cm^{-1} (medium) and 913 cm^{-1} (weak), a band at 757 cm^{-1} (strong) corresponding to W=O and a band at 536 cm^{-1} (strong) due to P-O bending. These bands can shift, weaken, strengthen, or mask in different conditions.

In Figure 5, compared with the initial Preyssler's structure, the bands arising from the synthesized nanocomposite changed obviously either in intensity or in position. Our findings show that many of the vibrational bands of Preyssler have blue-shifted and many of them have red-shifted, indicating that many of the bonds were strengthened and the others were weakened. As we can see, there is a significant shift in the W-O-W vibrations from 941 to 958 cm^{-1} and some displacements in the P-O stretchings from 1163 and 1079 cm^{-1} to 1156 and 1089 cm^{-1}, respectively. The characteristic band in 913 cm^{-1} is unchanged and the W=O band along with
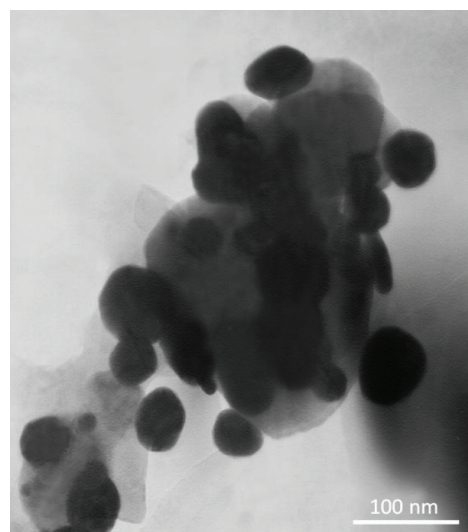
(a)
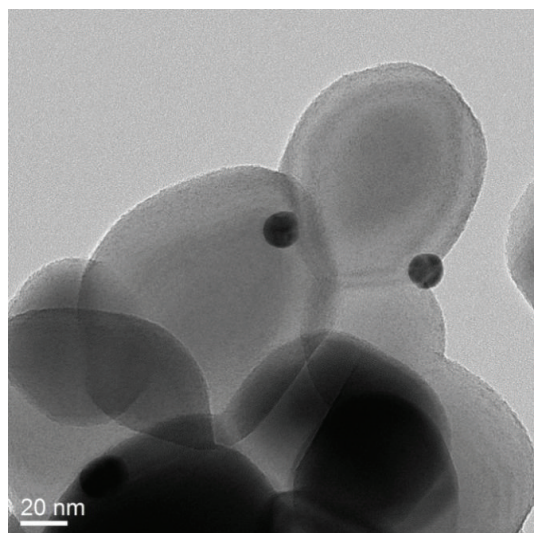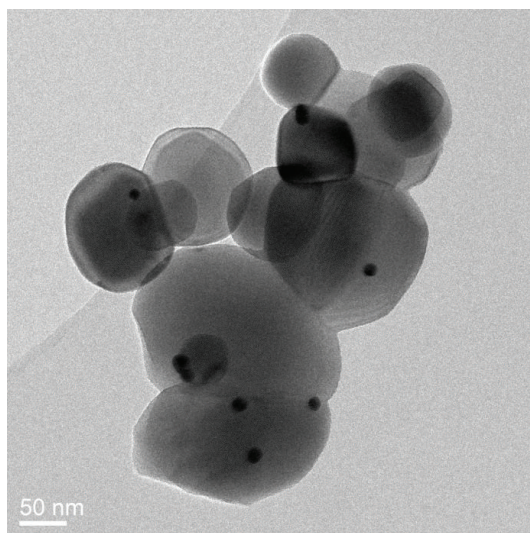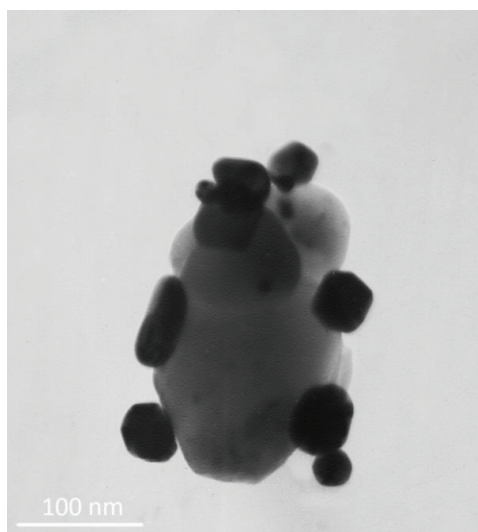
(b)

FIGURE 3: TEM images of Au/HP$_5$/TiO$_2$ (a) and Au/CsP$_5$/TiO$_2$ (b).

(a)

(b)

FIGURE 4: TEM images of Au/HP$_5$/NH$_2$-TiO$_2$ (a) and Au/CsP$_5$/NH$_2$-TiO$_2$ (b).

the P-O bending bands are overlapped by that of titanium dioxide. With respect to the PO$_4$ tetrahedrons vibrating almost independently from the rest of the anion, the significant blue shift of 17 cm^{-1} in the W-O-W vibrational mode suggests that Preyssler interacts strongly with the titanium dioxide surface and binds to it by the oxygen atoms in the W-O-W positions.

Titanium dioxide does not have significant bands between 800 and 1200 cm^{-1} and shows a broad band between 600 and 800 cm^{-1}. The W=O band placed in the 757 cm^{-1} is masked by that of titanium dioxide. These observations indicate that the Preyssler's anion chemically adsorbed onto the surface of titanium dioxide and interaction between Preyssler's anions and support mostly caused the distortion of anion and thus substantially not only weakened the IR vibrations covered up by the titanium dioxide background, but also caused some displacements in some bands. It is

completely common in IR spectra of polyoxometalates, when interacting with different counter ions [39]. Additionally, the organosilanes and amine groups characteristic peaks (2921, 1637, 1508, and 1458 cm^{-1}) in the FTIR spectra of the nanocomposites confirmed the presence of ligand on the surface.

Finally, XRD analysis confirmed the presence of gold nanoparticles and titanium dioxide in the synthesized nanocomposites (Figure 6).

The bleaching of the malachite green in a designed photoreactor was performed as a test reaction to estimate the catalytic activity of both synthesized nanocomposites (Au/CsP$_5$/-TiO$_2$ and Au/CsP$_5$/NH$_2$-TiO$_2$). We checked the intensity changes of UV band in malachite green in a photocatalytic reaction. Figure 7 summarizes UV-Vis results. It is clear that the photocatalytic activity strongly depends on the used catalyst.
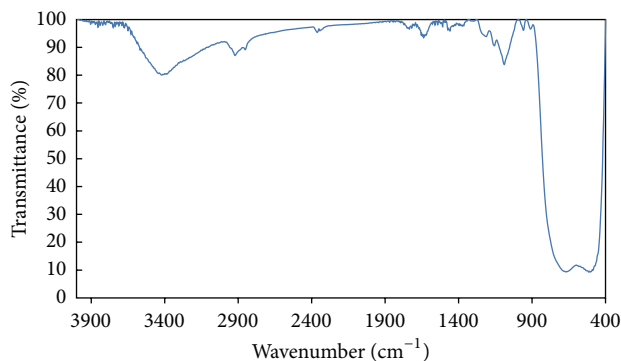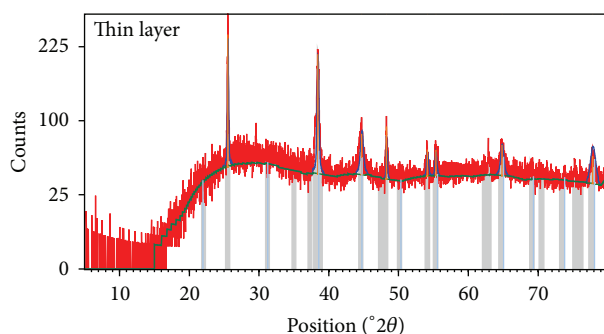
FIGURE 5: FTIR spectra of Au/Cs-P$_5$/NH$_2$-TiO$_2$.
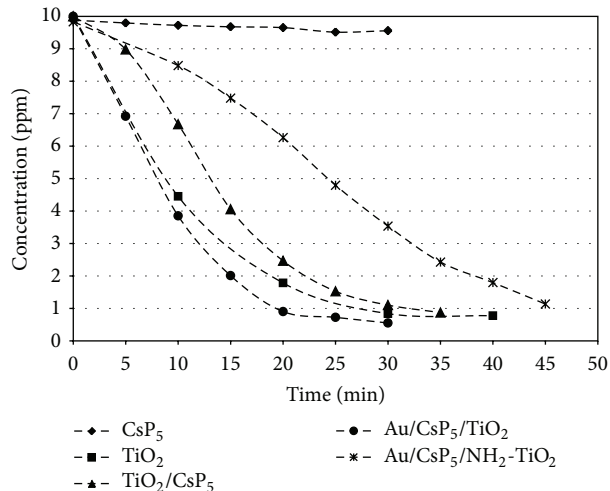

FIGURE 6: XRD pattern of Au/CsP$_5$/TiO$_2$.

FIGURE 7: Bleaching of malachite green in the presence of CsP$_5$, TiO$_2$, TiO$_2$/CsP$_5$, Au/CsP$_5$/TiO$_2$, and Au/CsP$_5$/NH$_2$-TiO$_2$.

As a control experiment series, in the same conditions we studied the bleaching of the dye in the presence of titanium dioxide, CsP$_5$, and titanium dioxide-CsP$_5$ (Figure 7). As we can see, there is an increase in photocatalytic activity, resulting in 100% bleaching of the dye after 20 minutes in the presence of Au/CsP$_5$/TiO$_2$. As expected, when Preyssler joins with titanium dioxide, photocatalytic activity is increased. It is suggested that CsP$_5$ as a cocatalyst can improve photocatalytic activity of titanium dioxide. The reduced photoactivity

of CsP$_5$-amine modified titanium dioxide-gold nanoparticles in Figure 7 can be attributed to higher gold loading in this nanocomposite, which might decrease the total effective titanium dioxide surface area during the bleaching of the dye. At the end of the reaction, the photocatalyst was filtered, washed, dried, and reused in another reaction. The recycled photocatalyst was used for three reactions without observation of appreciable loss in its catalytic activity. It is suggested that, because CsP$_5$ is not very soluble, it is present in the photocatalysts during the dye bleaching runs.

4. Conclusion

Green, eco-friendly, recyclable, and easily preparable cesium salt of Preyssler's anion is an efficient solid acid catalyst for the synthesis of gold nanoparticles as well as decoration of gold nanoparticles on the surface of titanium dioxide. Important features of this polyanion are high thermal and hydrolytic stability throughout a wide pH range. Thus, a wide range of chemical reactions can be affected without loss of structure or activity. Our findings show that counterions play an important role in the decoration of titanium dioxide, and Preyssler acts as a reducing agent and catalytic linker.
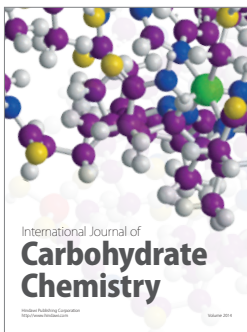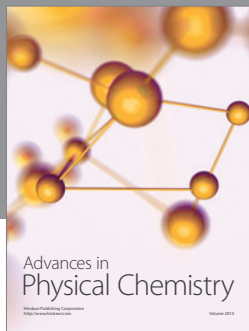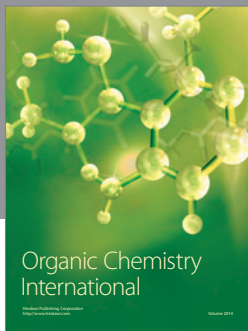
We observed that both of the synthesized nanocomposites with pure and modified titanium dioxide exhibit excellent photocatalytic activity in the bleaching of malachite green when exposed to UV irradiation. The remarkable bleaching of malachite green in the presence of these nanocomposites indicates that the treatments of other organic pollutants could be performed in the presence of this catalyst in order to obtain a perfect bleaching degree. This catalytic activity can also be extended to the other photocatalytic reactions.

References

[1] H. Yu, S. Zhang, H. Zhao, B. Xue, P. Liu, and G. Will, "High-performance TiO$_2$ photoanode with an efficient electron transport network for dye-sensitized solar cells," *Journal of Physical Chemistry C*, vol. 113, no. 36, pp. 16277–16282, 2009.

[2] H. Yu, S. Zhang, H. Zhao, and H. Zhang, "Photoelectrochemical quantification of electron transport resistance of TiO$_2$ photoanodes for dye-sensitized solar cells," *Physical Chemistry Chemical Physics*, vol. 12, no. 25, pp. 6625–6631, 2010.

[3] M. R. Hoffmann, S. T. Martin, W. Choi, and D. W. Bahnemann, "Environmental applications of semiconductor photocatalysis," *Chemical Reviews*, vol. 95, no. 1, pp. 69–96, 1995.

[4] A. Fujishima, K. Hashimoto, T. Iyoda, S. Fukayama, T. Yoshimoto, and T. Saitoh, US Patent US6939611, 2005.

[5] G. K. Mor, O. K. Varghese, M. Paulose, and C. A. Grimes, "A self-cleaning room temperature titania-nanotube hydrogen gas sensor," *Sensor Letters*, vol. 1, no. 1, pp. 42–46, 2003.

[6] E. Bessa, J. G. L. SantAnna, and M. J. Dezotti, "Photocatalysis: an approach to the treatment of oil field produced waters," *Journal of Advanced Oxidation Technologies*, vol. 4, no. 2, pp. 196–202, 1999.

[7] J. C. Cardoso, T. M. Lizier, and M. V. B. Zanoni, "Highly ordered TiO$_2$ nanotube arrays and photoelectrocatalytic oxidation of aromatic amine," *Applied Catalysis B*, vol. 99, no. 1-2, pp. 96–102, 2010.

[8] A. Hagfeldt and M. Gratzel, "Molecular photovoltaics," *Accounts of Chemical Research*, vol. 33, no. 5, pp. 269–277, 2000.

[9] M. Anpo, "Photocatalysis on titanium oxide catalysts: approaches in achieving highly efficient reactions and realizing the use of visible light," *Catalysis Surveys from Japan*, vol. 1, no. 2, pp. 169–179, 1997.

[10] D. R. Baker and P. V. Kamat, "Photosensitization of TiO_2 nanostructures with CdS quantum dots: particulate versus tubular support architectures," *Advanced Functional Materials*, vol. 19, no. 5, pp. 805–811, 2009.

[11] H. Kikuchi, M. Kitano, M. Takeuchi, M. Matsuoka, M. Anpo, and P. V. Kamat, "Extending the photoresponse of TiO_2 to the visible light region: photoelectrochemical behavior of TiO_2 thin films prepared by the radio frequency magnetron sputtering deposition method," *Journal of Physical Chemistry B*, vol. 110, no. 11, pp. 5537–5541, 2006.

[12] K. Wilke and H. D. Breuer, "The influence of transition metal doping on the physical and photocatalytic properties of titania," *Journal of Photochemistry and Photobiology A*, vol. 121, no. 1, pp. 49–53, 1998.

[13] P. Bouras, E. Stathatos, and P. Lianos, "Pure versus metal-ion-doped nanocrystalline titania for photocatalysis," *Applied Catalysis B*, vol. 73, no. 1-2, pp. 51–59, 2007.

[14] C. E. Gomez, J. R. V. Garcia, J. A. T. Antonio, M. A. C. Jacome, and C. A. J. Chavez, "Pt nanoparticles on titania nanotubes prepared by vapor-phase impregnation-decomposition method," *Journal of Alloys and Compounds*, vol. 495, no. 2, pp. 458–461, 2010.

[15] K. Nishijima, T. Fukahori, N. Murakami, T.-A. Kamai, T. Tsubota, and T. Ohno, "Development of a titania nanotube (TNT) loaded site-selectively with Pt nanoparticles and their photocatalytic activities," *Applied Catalysis A*, vol. 337, no. 1, pp. 105–109, 2008.

[16] Y. Yin, X. Tan, F. Hou, and L. Zhao, "Efficient synthesis of titania nanotubes and enhanced photoresponse of Pt decorated TiO_2 for water splitting," *Frontiers of Chemical Engineering in China*, vol. 3, no. 3, pp. 298–304, 2009.

[17] B.-L. He, B. Dong, and H.-L. Li, "Preparation and electrochemical properties of Ag-modified TiO_2 nanotube anode material for lithium-ion battery," *Electrochemistry Communications*, vol. 9, no. 3, pp. 425–430, 2007.

[18] I. Paramasivam, J. M. Macak, and P. Schmuki, "Photocatalytic activity of TiO_2 nanotube layers loaded with Ag and Au nanoparticles," *Electrochemistry Communications*, vol. 10, no. 1, pp. 71–75, 2008.

[19] L. P. An, X. P. Gao, G. R. Li, T. Y. Yan, H. Y. Zhu, and P. W. Shen, "Electrochemical lithium storage of titania nanotubes modified with NiO nanoparticles," *Electrochimica Acta*, vol. 53, no. 13, pp. 4573–4579, 2008.

[20] A. Kukovecz, M. Hodos, Z. Konya, and I. Kiricsi, "Complex-assisted one-step synthesis of ion-exchangeable titanate nanotubes decorated with CdS nanoparticles," *Chemical Physics Letters*, vol. 411, no. 4-6, pp. 445–449, 2005.

[21] A. Benoit, I. Paramasivam, Y.-C. Nah, P. Roy, and P. Schmuki, "Decoration of TiO_2 nanotube layers with WO_3 nanocrystals for high-electrochromic activity," *Electrochemistry Communications*, vol. 11, no. 4, pp. 728–732, 2009.

[22] M. A. Khan and O.-B. Yang, "Photocatalytic water splitting for hydrogen production under visible light on Ir and Co ionized titania nanotube," *Catalysis Today*, vol. 146, no. 1-2, pp. 177–182, 2009.

[23] M. Muruganandham, A. Ramakrishnan, Y. Kusumoto, and M. Sillanpää, "Are dopant-stabilized visible light-responsive photocatalysts efficient and stable?" *Physical Chemistry Physical Chemistry*, vol. 12, no. 44, pp. 14677–14681, 2010.

[24] A. Pearson, H. Jani, K. Kalantarzadeh, S. K. Bhargava, and V. Bansal, "Gold nanoparticle-decorated keggin ions/TiO_2 photococatalyst for improved solar light photocatalysis," *Langmuir*, vol. 27, no. 11, pp. 6661–6667, 2011.

[25] A. Pearson, S. K. Bhargava, and V. Bansal, "UV-switchable polyoxometalate sandwiched between TiO_2 and metal nanoparticles for enhanced visible and solar light photococatalysis," *Langmuir*, vol. 27, no. 15, pp. 9245–9252, 2011.

[26] K. Mori, K. Furubayashi, S. Okada, and H. Yamashita, "Synthesis of Pd nanoparticles on heteropolyacid-supported silica by a photo-assisted deposition method: an active catalyst for the direct synthesis of hydrogen peroxide," *RSC Advances*, vol. 2, no. 3, pp. 1047–1054, 2012.

[27] B. Keita, T. Liu, and L. Nadjo, "Synthesis of remarkably stabilized metal nanostructures using polyoxometalates," *Journal of Materials Chemistry*, vol. 19, no. 1, pp. 19–33, 2009.

[28] I. V. Kozhevnikov, "Catalysis by heteropoly acids and multicomponent polyoxometalates in liquid-phase reactions," *Chemical Reviews*, vol. 98, no. 1, pp. 171–198, 1998.

[29] N. Mizuno and M. Misono, "Heterogeneous catalysis," *Chemical Reviews*, vol. 98, no. 1, pp. 199–218, 1998.

[30] J. Liu, S. Liu, L. Qu, M. T. Pope, and C. Rong, "Derivatives of the 21-tungsto-9-antimonate heteropolyanion—part 1: inclusion of lanthanide cations," *Transition Metal Chemistry*, vol. 17, no. 4, pp. 311–313, 1992.

[31] J.-F. Liu, Y.-G. Chen, L. Meng, J. Guo, Y. Liu, and M. T. Pope, "Synthesis and characterization of novel heteropolytungstoarsenates containing lanthanides $[LnAs_4W_{40}O_{140}]^{25-}$ and their biological activity," *Polyhedron*, vol. 17, no. 9, pp. 1541–1546, 1998.

[32] M. H. Alizadeh, S. P. Harmalker, Y. Jeannin, J. Martin-Frere, and M. T. Pope, "A heteropolyanion with fivefold molecular symmetry that contains a nonlabile encapsulated sodium ion. The structure and chemistry of $[NaP_5W_{30}O_{110}]^{14-}$," *Journal of the American Chemical Society*, vol. 107, no. 9, pp. 2662–2669, 1985.

[33] F. F. Bamoharram, M. M. Heravi, M. Roshani, and N. Tavakoli, "N-oxidation of pyridine carboxylic acids using hydrogen peroxide catalyzed by a green heteropolyacid catalyst: preyssler's anion, $[NaP_5W_{30}O_{110}]^{14-}$," *Journal of Molecular Catalysis A*, vol. 252, no. 1-2, pp. 219–225, 2006.

[34] F. F. Bamoharram, M. M. Heravi, M. Roshani, M. Jahangir, and A. Gharib, "Preyssler catalyst, $[NaP_5W_{30}O_{110}]^{14-}$: a green, efficient and reusable catalyst for esterification of salicylic acid with aliphatic and benzylic alcohols," *Applied Catalysis A*, vol. 302, no. 1, pp. 42–47, 2006.

[35] F. F. Bamoharram, "Role of polyoxometalates as green compounds in recent developments of nanoscience," *Synthesis and Reactivity in Inorganic, Metal-Organic and Nano-Metal Chemistry*, vol. 41, no. 8, pp. 893–922, 2011.

[36] A. Ayati, A. Ahmadpour, F. F. Bamoharram, M. M. Heravi, and H. Rashidi, "Photocatalytic synthesis of gold nanoparticles using preyssler acid and their photocatalytic activity," *Chinese Journal of Catalysis*, vol. 32, no. 6, pp. 978–982, 2011.

[37] G. Sun, Q. Li, R. Xu, J. Gu, M. Ju, and E. Wang, "Controllable fabrication of platinum nanospheres with a polyoxometalate-assisted process," *Journal of Solid State Chemistry*, vol. 183, no. 11, pp. 2609–2615, 2010.

[38] X. K. Fu, J. R. Chen, L. Q. Li, Q. Wang, and Y. Sui, "Organophos-phonotungstic HPA of Keggin type with sulfo, taurine and glycine substituted ethylphosphonic acids as the coordinate center," *Chinese Chemical Letters*, vol. 14, no. 5, pp. 515–518, 2003.

[39] F. F. Bamoharram, "Vibrational spectra study of the interactions between keggin heteropolyanions and amino acids," *Molecules*, vol. 14, no. 9, pp. 3214–3221, 2009.